

Genes Involved in Long-Chain Alkene Biosynthesis in *Micrococcus luteus*[▽]

Harry R. Beller,^{1,2†*} Ee-Been Goh,^{1,3†} and Jay D. Keasling^{1,3,4}

Joint BioEnergy Institute, 5885 Hollis Street, Emeryville, California 94608¹; Earth Sciences Division, Lawrence Berkeley National Laboratory, Berkeley, California 94720²; Physical Biosciences Division, Lawrence Berkeley National Laboratory, Berkeley, California 94720³; and Departments of Chemical Engineering and of Bioengineering, University of California, Berkeley, California 94720⁴

Received 24 September 2009/Accepted 12 December 2009

Aliphatic hydrocarbons are highly appealing targets for advanced cellulosic biofuels, as they are already predominant components of petroleum-based gasoline and diesel fuels. We have studied alkene biosynthesis in *Micrococcus luteus* ATCC 4698, a close relative of *Sarcina lutea* (now *Kocuria rhizophila*), which 4 decades ago was reported to biosynthesize *iso*- and *anteiso*-branched, long-chain alkenes. The underlying biochemistry and genetics of alkene biosynthesis were not elucidated in those studies. We show here that heterologous expression of a three-gene cluster from *M. luteus* (Mlut_13230-13250) in a fatty acid-overproducing *Escherichia coli* strain resulted in production of long-chain alkenes, predominantly 27:3 and 29:3 (no. carbon atoms: no. C=C bonds). Heterologous expression of Mlut_13230 (*oleA*) alone produced no long-chain alkenes but unsaturated aliphatic monoketones, predominantly 27:2, and *in vitro* studies with the purified Mlut_13230 protein and tetradecanoyl-coenzyme A (CoA) produced the same C₂₇ monoketone. Gas chromatography-time of flight mass spectrometry confirmed the elemental composition of all detected long-chain alkenes and monoketones (putative intermediates of alkene biosynthesis). Negative controls demonstrated that the *M. luteus* genes were responsible for production of these metabolites. Studies with wild-type *M. luteus* showed that the transcript copy number of Mlut_13230-13250 and the concentrations of 29:1 alkene isomers (the dominant alkenes produced by this strain) generally corresponded with bacterial population over time. We propose a metabolic pathway for alkene biosynthesis starting with acyl-CoA (or-ACP [acyl carrier protein]) thioesters and involving decarboxylative Claisen condensation as a key step, which we believe is catalyzed by OleA. Such activity is consistent with our data and with the homology (including the conserved Cys-His-Asn catalytic triad) of Mlut_13230 (OleA) to FabH (β-ketoacyl-ACP synthase III), which catalyzes decarboxylative Claisen condensation during fatty acid biosynthesis.

Aliphatic hydrocarbons are favorable targets for advanced cellulosic biofuels, as they are already predominant components of petroleum-based gasoline and diesel fuels and thus would be compatible with existing engines and fuel distribution systems. Certain bacteria are promising sources of the enzymes necessary for conversion of saccharification products such as glucose to aliphatic hydrocarbons, as a number of strains capable of aliphatic hydrocarbon production have been reported (12). Although some of these reports have proven irreproducible and are in question (e.g., see reference 22), alkene biosynthesis was well documented in *Sarcina lutea* ATCC 533 (now *Kocuria rhizophila*), which 4 decades ago was reported by two research groups to biosynthesize *iso*- and *anteiso*-branched, long-chain (primarily C₂₅ to C₂₉) alkenes (2, 3, 21). The biosynthetic pathway was postulated to involve decarboxylation and condensation of fatty acids; however, the underlying biochemistry and genetics of alkene biosynthesis were not elucidated. We chose to study alkene biosynthesis in *Micrococcus luteus* ATCC 4698 (also NCTC 2665), a close relative of *S. lutea* for which a genome sequence is available (24) and in which we have observed long-chain alkene biosynthesis. In this article, we provide *in vivo* and *in vitro* evidence of proteins in

M. luteus that catalyze production of long-chain alkenes (and a key alkene biosynthesis intermediate, a long-chain monoketone) when expressed heterologously in *Escherichia coli* and also report how expression of the three relevant genes relates to growth and alkene production in wild-type *M. luteus*.

MATERIALS AND METHODS

Bacterial strains, plasmids, oligonucleotides, and reagents. Bacterial strains and plasmids used in this study are listed in Table 1. Plasmid extractions were carried out using the Qiagen (Valencia, CA) miniprep and midprep kits. Oligonucleotides were designed using the web-based PrimerBlast program (http://www.ncbi.nlm.nih.gov/tools/primer-blast/index.cgi?LINK_LOC=BlastHomeAd) and synthesized by Integrated DNA Technologies (San Diego, CA) or Bioneer (Alameda, CA). *M. luteus* locus tags (e.g., Mlut_13230) used in Table 1 and elsewhere in this article correspond to the whole-genome sequence available in the GenBank/EMBL database under accession no. CP001628.

Media and bacterial growth. *E. coli* was propagated as previously described (17), whereas *M. luteus* was propagated at 30°C in tryptic soy broth or on tryptic soy agar plates.

For most *M. luteus* studies described here and for studies of heterologous gene expression in *E. coli* DH1 strains, cells were grown in 15 ml of tryptic soy broth in a 30-ml glass tube with 200 rpm agitation at 30°C for up to 60 h before being harvested for analysis. Cultures grown for protein purification were cultivated with an autoinduction medium containing Luria-Bertani broth, phosphate buffer, and carbon sources as described by Studier (19).

When required, antibiotics were added to the growth medium at the following final concentrations: chloramphenicol, 25 μg/ml; kanamycin, 50 μg/ml (100 μg/ml when autoinduction medium was used). A final concentration of 0.5 mM isopropyl-β-D-thiogalactopyranoside (IPTG) was added to media when induction of genes was required.

Plasmids and strain construction for heterologous expression in *E. coli*. To clone *M. luteus* genes into expression plasmids, genomic DNA was first isolated using

* Corresponding author. Mailing address: Joint BioEnergy Institute, 5885 Hollis Street, Emeryville, CA 94608. Phone: (510) 486-7321. Fax: (510) 486-5686. E-mail: HRBeller@lbl.gov.

† H.R.B. and E.-B.G. contributed equally to this study.

▽ Published ahead of print on 28 December 2009.

TABLE 1. Bacterial strains and plasmids used in this study

Strain or plasmid	Relevant characteristic(s)	Source or reference
<i>E. coli</i> strains		
BL21(DE3)	F ⁻ <i>ompT gal dcm lon hsdSB</i> (r _B ⁻ m _B ⁻) λ(DE3)	20
DH1	<i>endA1 recA1 gyrA96 thi-1 glnV44 relA1 hsdR17</i> (r _K ⁻ m _K ⁺) λ ⁻	13
LT-Δ <i>fadE</i>	DH1 Δ <i>fadE</i> with pKS1	18
EGS084	LT-Δ <i>fadE</i> with pEC-XK99E	This study
EGS145	LT-Δ <i>fadE</i> with pEG142	This study
EGS180	LT-Δ <i>fadE</i> with pEG174	This study
EGS210	LT-Δ <i>fadE</i> with pEG200	This study
EGS212	LT-Δ <i>fadE</i> with pEG205	This study
EGS220	BL21(DE3) with pEG185	This study
EGS244	LT-Δ <i>fadE</i> with pEG225	This study
EGS300	LT-Δ <i>fadE</i> with pEG275	This study
<i>Micrococcus luteus</i> ATCC 4698	Wild type	ATCC
Plasmids		
pEC-XK99E	Km ^r ; <i>E. coli</i> - <i>C. glutamicum</i> shuttle expression vector with ColE1 origin of replication and <i>trc</i> promoter	11
pKS1	Cm ^r ; p15a derivative containing ' <i>tesA</i> ^a ' under the <i>lacUV5</i> promoter	18
pSKB3	Km ^r ; derivative of expression vector pET-28a with the thrombin protease site replaced by a TEV protease site	Stephen K. Burley
pEG142	Km ^r ; ~5.2 kb containing <i>Mlut_13230-13250</i> cloned into pEC-XK99E at KpnI and XbaI sites	This study
pEG174	Km ^r ; ~1 kb containing <i>Mlut_13230 #1</i> into pEC-XK99E at EcoRI and XbaI sites	This study
pEG185	Km ^r ; ~1-kb fragment of <i>Mlut_13230 #2</i> cloned into pSKB3 at NdeI and SalI sites	This study
pEG200	Km ^r ; ~1.2-kb fragment of <i>Mlut_09290</i> cloned into pEC-XK99E at EcoRI and XbaI sites	This study
pEG205	Km ^r ; ~1-kb fragment of <i>Mlut_09310</i> cloned into pEC-XK99E at EcoRI and XbaI sites	This study
pEG225	Km ^r ; ~3-kb fragment of <i>Mlut_13240</i> cloned into pEC-XK99E at XbaI site	This study
pEG275	Km ^r ; ~1.1-kb fragment of <i>Mlut_13250</i> cloned into pEC-XK99E at XbaI and SbfI sites	This study

^a '*tesA*, *tesA* thioesterase gene from *E. coli* from which the region encoding the leader sequence has been removed.

the Genomic-DNA tips and Genomic DNA buffer set from Qiagen and used as the template for PCR amplification of the genes of interest. To reduce error rates in the DNA amplification reaction, Phusion DNA polymerase (Finnzymes, Woburn, MA) was used. In addition, due to the high-GC (73%) DNA content of *M. luteus*, 10% dimethyl sulfoxide (DMSO) was included in the PCR mixture to eliminate any secondary structure of the template. For templates that were more difficult to amplify, 1 M (final concentration) betaine was used instead of DMSO. All primers used to amplify target genes are listed in Table 2. PCR products and plasmid DNA were digested with the appropriate restriction enzymes and purified with QIAquick gel extraction and/or PCR purification kits (Qiagen) before being ligated and transformed into *E. coli*. Proper clone construction was confirmed by DNA sequencing, which was performed by Quintara Biosciences (Berkeley, CA). Expression of *M. luteus* genes in constructs was confirmed by extraction of proteins, tryptic digestion, and analysis of the resulting peptides by electrospray ionization liquid chromatography-tandem mass spectrometry (LC/MS/MS) (QSTAR Elite Hybrid Quadrupole TOF; Applied Biosystems).

Purification of N-terminally His-tagged *Mlut_13230* protein for *in vitro* assays. *E. coli* strain EGS220 (Table 1) was grown at 30°C in 200 ml of autoinduction medium for 20 to 24 h before being harvested for protein purification. Cell lysis and protein purification were carried out as described elsewhere (15), with a few modifications. Briefly, the harvested cell pellet was resuspended in 50 mM Tris-Cl (pH 8.0) with 10% glycerol, 500 mM NaCl, 30 mM imidazole, and 5 mM dithiothreitol (DTT). Cells were lysed by sonication, followed by three freeze-thaw cycles at -80°C in the presence of 1 mg/ml lysozyme and 0.1% Triton X-100. Clarified cell lysates were incubated with Ni-nitrilotriacetic acid resin at 4°C for 1 h with gentle rocking before being applied to a gravity flow column. The column was washed with 50 mM Tris-Cl (pH 7.9) containing 10% glycerol, 500 mM NaCl, 30 mM imidazole, and 5 mM DTT, and proteins were eluted with the same buffer except that the imidazole concentration was increased to 200 mM. Eluted proteins were concentrated and exchanged with 100 mM potassium phosphate buffer (pH 7.0) with 25 mM NaCl using Amicon Centrifugal Devices (Millipore). Purified proteins were run on an 8 to 16% gradient sodium dodecyl sulfate-polyacrylamide gel electrophoresis gel, stained with Coomassie blue dye, and observed to contain a major band at ~40 kDa. This band was excised, an in-gel trypsin digest was performed, and the digested peptides were analyzed by electrospray ionization LC/MS/MS (QSTAR Elite

Hybrid Quadrupole TOF; Applied Biosystems) to confirm that the 40-kDa protein band corresponded to the *Mlut_13230* protein. In-solution trypsin digests carried out on purified OleA samples determined that OleA constituted at least 70 to 75% of the protein based upon calculations using the exponentially modified protein abundance index method (9).

***In vitro* assays with purified *Mlut_13230*.** Assays (500-μl total volume) were conducted in 4-ml screw-cap glass vials with polytetrafluoroethylene (PTFE)-lined septa. Assay mixtures contained 1 mM myristoyl-coenzyme A (CoA) (Sigma), 100 μl freshly purified *Mlut_13230* protein (2 to 4 mg/ml), and freshly prepared *E. coli* DH1 (wild-type) cell lysate in 0.1 M potassium phosphate buffer (pH 7.0) containing 5 mM DTT. Preparation of cell lysates was performed as follows. Ten milliliters of *E. coli* DH1 was grown overnight in LB at 37°C before being harvested by centrifugation. Cell pellets were washed once with 0.1 M potassium phosphate buffer (pH 7.0) and resuspended in 750 μl of the same phosphate buffer before being subjected to cell lysis by sonication. Cell lysate was clarified by centrifugation, and the supernatant was used for the *in vitro* assay.

Controls included assay mixtures without *Mlut_13230* protein or without DH1 cell lysate. Assay vials were gently shaken for 1.5 h at 30°C. After incubation, assay mixtures were extracted with high-purity hexane (OmniSolv; EMD Chemicals) that was amended with two internal standards: decane-*d*₂₂ and tetracosane-*d*₅₀ (each at a final concentration of 40 ng/μl for gas chromatography/mass spectrometry [GC/MS] analysis). One milliliter of hexane was added to the assay solution, mixed well, and allowed to sit for 30 min, and the vials were centrifuged at 2,000 rpm for 10 min (20°C) in an Allegra 25R centrifuge with an A14 rotor (Beckman Coulter). The extraction step was repeated, the two 1-ml aliquots of hexane were combined, and the extracts were derivatized with ethereal diazomethane (5, 6) with high-purity diethyl ether (>99.8% purity, preserved with 2% ethanol; Fluka) and concentrated under a gentle stream of ultrahigh-purity N₂ to 50 μl for analysis by GC/MS. Throughout the procedure, the hexane contacted only glass or PTFE.

Extraction of long-chain aliphatic hydrocarbons and related metabolites from bacterial cultures. Fifteen-milliliter cultures (either *E. coli* constructs or wild-type *M. luteus*) in 30-ml glass tubes with PTFE-lined screw-cap closures were centrifuged at 3,500 rpm for 15 min (20°C) in an Allegra 25R centrifuge with an A14 rotor, and the aqueous phase was decanted. The pellet was amended with 100 μl of reagent water, and the mixture was homogenized with a vortex mixer. Then, 1 ml of high-purity methanol (B&J Brand, ≥99.9% purity) and 4 ml

TABLE 2. Primers used in this study

Primer use and target gene(s)	Primer name	Sequence ^a (5'→3')
Gene amplification		
Mlut_13230 #1	MLprimer_F1 MLprimer_R1	TACTGAATT <u>CGAAGGAGGGTCTGGTGACGAACGTGT</u> TTCATCTAG <u>ACCCACTAGTTGGCTCCTTCAGC</u>
Mlut_13230-13250	MLprimer_F2 MLprimer_R2	AGAC <u>ACTAGTAGGAGGATTGGTCTGGTGACGAACG</u> ATCTCTAGAGTTTCCCGAACGAAAGCTC
Mlut_09290	MLprimer_F3 MLprimer_R3	CATGGAATTCAGACCCAGAGGCAGCAGACC GCC <u>ACTAGTCTCCGGCTCAGACGCTGC</u>
Mlut_09310	MLprimer_F4 MLprimer_R4	CATGGAATTCGGCAGAGAGAGGCACCATGA GCC <u>ACTAGTGTACGTGGACAGTGAATCAGACGG</u>
Mlut_13230 #2	MLprimer_F5 MLprimer_R5	TCACATATGGTGACGAACGTGTCCGGCAA AGTGT <u>CGACTTGGCTCCTTCAGCTACCA</u>
Mlut_13240	MLprimer_F6 MLprimer_R6	CTATACTAGTGCTCGAGATCGAATGGTGAGCTGAAGG ATCATCTAGAGTCGAGGCCGACGTCGTAGCCGAAG
Mlut_13250	MLprimer_F7 MLprimer_R7	GATTTCTAGACGCCGGCGGGAAGGTGGGTG AAGTCTGCAGGGGACGGGCGCTCGTTCCGGC
Real-time PCR		
Mlut_13230	qPCR_MLprimer_F1 qPCR_MLprimer_R1	CCTGATCAAGGACGGTCTCG CTGGTGGGTGATGAATCGTG
Mlut_13240	qPCR_MLprimer_F2 qPCR_MLprimer_R2	ACACCGACCAGCAGAGCAAG GTGGTGATCACGTGCTGGAG
Mlut_13250	qPCR_MLprimer_F3 qPCR_MLprimer_R3	AGTACGAGGCCGTGAACGTG GGGAGGAGACGTGGACGAAG

^a Underlined sequences indicate restriction sites used for cloning purposes.

high-purity hexane were added to the cells; as discussed previously, the hexane was amended with perdeuterated alkane standards to assess sample-specific analytical recovery. The cell-solvent mixture was homogenized with a vortex mixer and sonicated in an ice bath for 15 min, allowed to sit for 10 min, and then centrifuged at 3,500 rpm for 15 min (20°C). The hexane layer was then removed with a solvent-cleaned Pasteur pipette and transferred to a glass 10-ml conical vial. The hexane was concentrated to 100 μ l under a gentle stream of ultrahigh-purity N₂; 50 μ l was transferred (*via* 100- μ l gas-tight glass syringe) to a vial for GC/MS analysis, and the remaining 50 μ l was derivatized with ethereal diazomethane (as discussed previously) and then concentrated to 50 μ l for GC/MS analysis. *M. luteus* extracts were not derivatized. As discussed for the *in vitro* assay extractions, organic solvents contacted only glass or PTFE, and all glass and PTFE surfaces were rigorously precleaned with high-purity acetone.

Analysis by GC/MS (quadrupole and time of flight, or TOF). For electron ionization (EI) GC/MS analyses with a quadrupole mass spectrometer, studies were performed with a model 7890A GC (Agilent) with a DB-5 fused silica capillary column (30-m length, 0.25-mm inner diameter, 0.25- μ m film thickness; J & W Scientific) coupled to an HP 5975C series mass selective detector; 1- μ l injections were performed by a model 7683B autosampler. The GC oven was typically programmed from 40°C (held for 3 min) to 300°C at 15°C/min and then held for 20 min; the injection port temperature was 250°C, and the transfer line temperature was 280°C. The carrier gas, ultrahigh-purity helium, flowed at a constant rate of 1 ml/min. Injections were splitless, with the split turned on after 0.5 min. For full-scan data acquisition, the MS typically scanned from *m/z* 50 to 600 at a rate of 2.7 scans/s. Selected ion monitoring (SIM) acquisition was used for certain studies when additional sensitivity was required; specific ions monitored for SIM are discussed in Results, when applicable.

Selected samples were subjected to GC-TOF analysis to confirm the elemental composition of key metabolic products. GC-chemical ionization (CI)-TOF analyses were performed with a Waters/MicroMass GCT instrument scanning from *m/z* 65 to 800 with GC conditions as described previously; positive-ion CI mode was used, and the reagent gas was methane. GC-EI-TOF analyses were carried

out with a Waters GCT Premier instrument scanning from *m/z* 35 to 650 (with dynamic range enhancement) with GC conditions as described previously. Elemental compositions were calculated with MassLynx software.

Transcriptional studies of *M. luteus* with reverse transcription-quantitative PCR (RT-qPCR) analysis. For transcriptional studies, RNA in *M. luteus* cultures was preserved immediately before harvesting by adding an ethanol solution containing 5% phenol. Extraction and purification of RNA were carried out with Qiagen RNeasy kits. Concentration and integrity of RNA were determined with a Thermo Scientific Nanodrop ND-1000 spectrophotometer and an Agilent 2100 BioAnalyzer, respectively.

Synthesis of cDNA for RT-qPCR analysis was carried out using 2 μ g of total RNA primed with 10 μ g of random hexamers and reverse transcribed using SuperScript III enzyme (Invitrogen, Carlsbad, CA). The RT reaction was carried out for 2 h at 50°C before the RNA was hydrolyzed with 2 U of RNase H (Invitrogen) at 37°C for 30 min. qPCR analyses were then conducted with an Applied Biosystems StepOne system using 2 μ l of the RT reaction mixture, gene-specific primers (Table 2), and the PerfeCTa SYBR green FastMix (Quanta Biosciences). qPCR cycle parameters were as follows: initial denaturation at 95°C for 10 min, followed by 40 cycles of 15 s denaturation at 95°C and 1 min annealing and extension at 60°C. Fluorescence measurements were taken between cycles. At the conclusion of the qPCR cycle, melting curve analysis was conducted by denaturing the PCR products from 60°C to 95°C and making fluorescence measurements at 0.3°C increments. All reactions were performed in duplicate. Transcripts were quantified with reference to a standard curve generated by serial dilution of pEG142 (from 10⁵ to 10¹⁰ copies/reaction).

RESULTS

Identification of condensing enzymes as potential candidates for a key alkene biosynthesis step. After unsuccessful

attempts to identify candidate genes for alkene biosynthesis *via* transcriptomics in *M. luteus* (not addressed in this article), we drew upon findings of previous *S. lutea* research and hypothesized that enzymes catalyzing fatty acid decarboxylation and condensation would play an important role in alkene biosynthesis. Specifically, some important observations for *S. lutea* were that (i) the dominant alkenes in *S. lutea*, namely, *iso*- and *anteiso*-branched C₂₉ monoalkenes with the double bond near the center (at C-13), are very plausibly derived from decarboxylation and “head-to-head” condensation of the dominant fatty acids in that bacterium, namely, *iso*- and *anteiso*-branched C₁₅ saturated acids (1, 2) and (ii) *in vitro* studies with cell-free *S. lutea* extracts, palmitate-16-¹⁴C, palmitate-1-¹⁴C, and their CoA derivatives indicated that decarboxylation of acyl-CoAs was important in alkene biosynthesis (3).

Based upon these observations for *S. lutea*, we hypothesized that homologs of “condensing enzymes” involved in fatty acid biosynthesis [i.e., β-ketoacyl-ACP (acyl carrier protein) synthases] could be involved in alkene biosynthesis from fatty acids, as these enzymes catalyze decarboxylation of activated aliphatic acids (malonyl-ACP) and nucleophilic attack by the resulting carbanion on an acyl-CoA or acyl-ACP thioester (Claisen condensation) (8, 23).

A search of the draft genome sequence of *M. luteus* for genes associated with fatty acid metabolism revealed three possible condensing enzymes: Mlut_09290 (β-ketoacyl-ACP synthase II or FabF), Mlut_09310 (β-ketoacyl-ACP synthase III or FabH), and Mlut_13230 (a possible FabH homolog). Alignments of the translated products of these three genes and the most similar sequences from *E. coli* and two sequenced, Gram-positive, close relatives of *M. luteus* (*Arthrobacter aurescens* TC1 and *Arthrobacter* sp. strain FB24) revealed the presence of three key conserved, active-site residues characteristic of condensing enzymes (23) in all sequences (Fig. 1): Cys-His-Asn for the FabH homologs (Mlut_09310 and Mlut_13230) and Cys-His-His for the FabF homolog (Mlut_09290). Furthermore, based on their gene neighborhood, it seems likely that Mlut_09290 and Mlut_09310 are, respectively, *fabF* and *fabH*, which encode key condensing enzymes involved in fatty acid biosynthesis; the six-gene cluster containing Mlut_09310 and Mlut_09290 includes a number of other genes critical to biosynthesis of branched-chain fatty acids, including a putative branched-chain α-keto acid decarboxylase (Mlut_09340), malonyl-CoA:ACP transacylase (*fabD*; Mlut_09320), and ACP (Mlut_09300). In addition, it is clear from Fig. 1 that Mlut_09310 and Mlut_09290 have relatively high sequence identity to known copies of FabH and FabF, respectively, in contrast to Mlut_13230, which has relatively low sequence identity to *E. coli* FabH.

Thus, the putative condensing enzymes Mlut_09290, Mlut_09310, and Mlut_13230 were selected as candidates for catalyzing an important reaction in alkene biosynthesis.

Long-chain alkenes and unsaturated monoketones resulting from heterologous expression of *M. luteus* condensing enzymes (and associated genes) in fatty acid-overproducing *E. coli*. To test the hypothesis that one or more of the putative condensing enzymes in *M. luteus* has a role in alkene biosynthesis, we expressed Mlut_13230, Mlut_09290, and Mlut_09310 in a fatty acid-overproducing *E. coli* strain (strains EGS180, EGS210, and EGS212, respectively; Table 1) and analyzed the metabo-

lites by GC/MS. Comparison of total ion chromatograms (TIC) from extracts of strains EGS210 and EGS212 with those of a negative control (empty vector; strain EGS084; Table 1) did not reveal any new peaks resulting from the presence of Mlut_09290 or Mlut_09310 (data not shown). However, the TIC representing strain EGS180 did reveal some noteworthy peaks relative to the negative control (peaks labeled 27:2, 27:1, 29:2, and 29:1 in Fig. 2A; these labels represent X:Y, where X = carbon number and Y = number of C=C bonds). The 27:2 peak was particularly prominent. The TIC in Fig. 2A represents an extract derivatized with diazomethane. The extracts were derivatized to reduce baseline noise by converting abundant and strongly tailing free fatty acids to fatty acid methyl esters, which were well resolved chromatographically and had minimal tailing. The labeled peaks in Fig. 2A were also present in the TIC of underivatized samples but were less prominent (e.g., Fig. 2B); thus, derivatization did not create these compounds but merely enhanced their detectability. Mass spectra of these peaks (e.g., Fig. 3A) were consistent with mono- and diunsaturated C₂₇ and C₂₉ monoketones, as the nominal molecular ions for peaks 27:2, 27:1, 29:2, and 29:1 were at *m/z* 390 (C₂₇H₅₀O), 392 (C₂₇H₅₂O), 418 (C₂₉H₅₄O), and 420 (C₂₉H₅₆O), respectively. Although authentic standards are not available for these compounds, GC-EI-TOF and GC-CI-TOF analyses confirmed the elemental compositions just described. For the 27:2, 27:1, 29:2, and 29:1 monoketones, measured masses agreed with the calculated masses within a 0.4-mDa absolute error and a 1.0-ppm relative error.

Because C₂₇ and C₂₉ unsaturated monoketones are plausible intermediates in a hypothesized pathway of alkene biosynthesis from C₁₄ and C₁₆ fatty acids (see Discussion), we further pursued the possible role of Mlut_13230 in alkene biosynthesis. We constructed a plasmid containing the native three-gene cluster that includes Mlut_13230 (i.e., Mlut_13230-13250) and expressed it in a fatty acid-overproducing *E. coli* strain (strain EGS145; Table 1). GC/MS analysis of the extract from strain EGS145 revealed peaks in the TIC that were not present in strain EGS180 (with Mlut_13230 alone) or in the negative control (strain EGS084) (Fig. 2B). Mass spectra of these peaks (e.g., Fig. 3B) were consistent with di- and triunsaturated C₂₇ and C₂₉ alkenes, as the nominal molecular ions for peaks 27:3, 27:2, 29:3, and 29:2 were at *m/z* 374 (C₂₇H₅₀), 376 (C₂₇H₅₂), 402 (C₂₉H₅₄), and 404 (C₂₉H₅₆), respectively. Authentic standards are not commercially available for di- and triunsaturated C₂₇ and C₂₉ alkenes. However, for the most abundant ions in these spectra (dominated by a series of ions differing by 14 atomic mass units or CH₂ groups), fragmentation patterns were consistent with National Institute of Standards and Technology library spectra of shorter alkenes for which standards are available; for example, the best library match for the spectrum of the peak labeled 27:3 was a shorter triunsaturated alkene (22:3). Furthermore, GC-EI-TOF analyses confirmed the elemental compositions just described. For the 27:3, 27:2, and 29:3 alkenes, measured masses agreed with the calculated masses within a 0.3-mDa absolute error and a 0.8-ppm relative error (for the 29:2 alkene, these errors were 1.0 mDa and 2.5 ppm, respectively). The total concentration of the four alkenes was on the order of 40 μg/liter (a 14:1 alkene standard was used for this estimate, as authentic standards were not commercially available).

In Fig. 2B, there are two peaks in the EGS180 extract

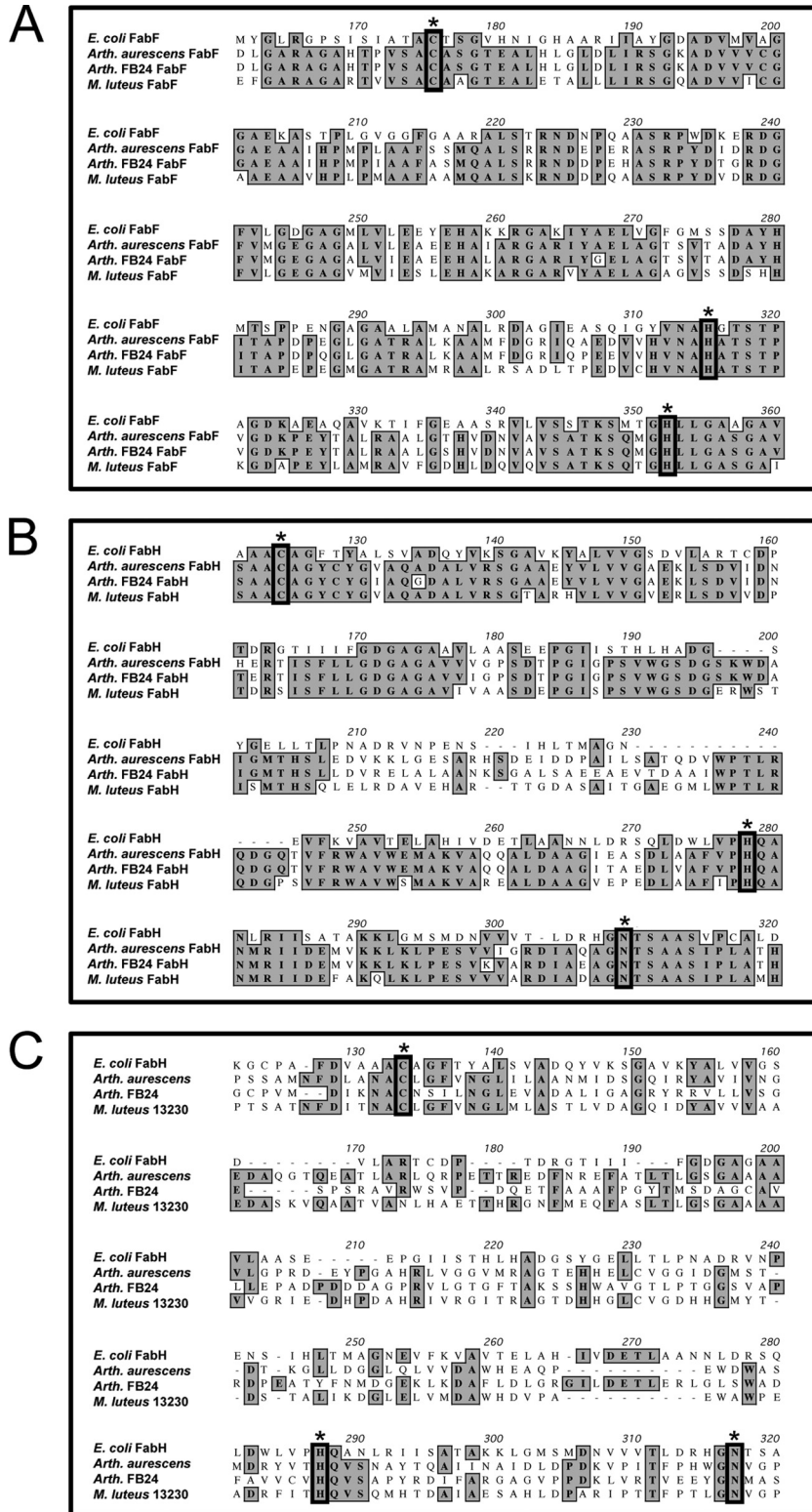


FIG. 1. Partial amino acid alignments of three translated *M. luteus* genes with homology to condensing enzymes involved in fatty acid biosynthesis: (A) Mlut_09290 (FabF), (B) Mlut_09310 (FabH), and (C) Mlut_13230. Alignments include the most similar sequences from *E. coli* and close relatives *Arthrobacter* sp. strain FB24 and *Arthrobacter aureus* TC1. Three conserved active-site residues (see text) are highlighted: Cys-His-His (panel A) or Cys-His-Asn (panels B and C). Gray areas indicate sequence identity. (A) GenBank accession numbers: *E. coli*, NP_415613; strain TC1, YP_948166; strain FB24, YP_831948. (B) GenBank accession numbers: *E. coli*, NP_415609; strain TC1, YP_948164; strain FB24, YP_831946. (C) GenBank accession numbers: *E. coli*, NP_415609; strain TC1, YP_947743; strain FB24, YP_832433.

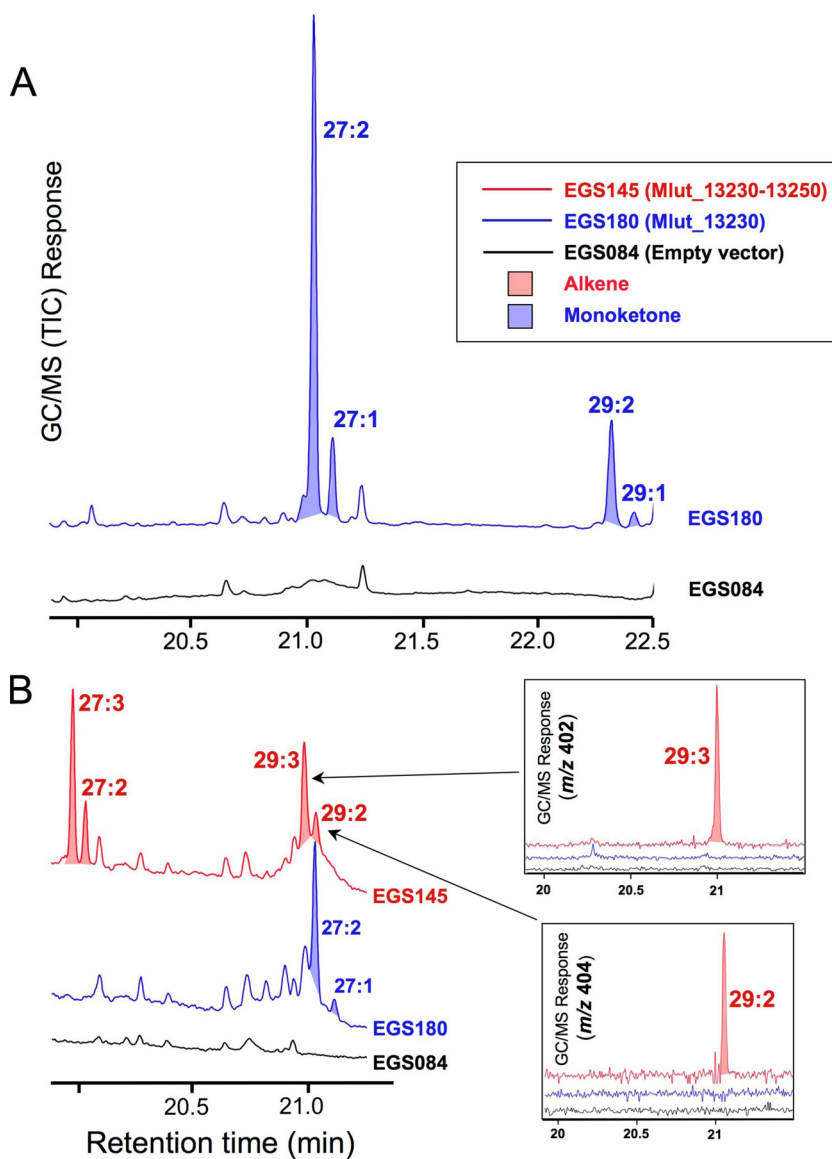


FIG. 2. (A) TIC of diazomethane-derivatized extracts of fatty acid-overproducing *E. coli* expressing Mlut_13230 (strain EGS180; blue) or no *M. luteus* genes (strain EGS084; black). Long-chain ketones (27:2, 27:1, 29:2, 29:1; blue fill) were observed when Mlut_13230 was expressed and were not observed in the control. (B) TIC of underivatized extracts of fatty acid-overproducing *E. coli* expressing Mlut_13230-13250 (strain EGS145; red), Mlut_13230 (strain EGS180; blue), or no *M. luteus* genes (strain EGS084; black). Long-chain alkenes (27:3, 27:2, 29:3, 29:2; red fill) were observed only when Mlut_13230-13250 were present and were not observed with Mlut_13230 alone or in the negative control. There are peaks from strain EGS180 that coelute with 29:3 and 29:2 alkenes; however, inspection of extracted ion profiles for the molecular ions of these alkenes (m/z 402 and 404) demonstrates that the alkenes are not present in strain EGS180 (insets).

(Mlut_13230 only) that coelute with the peaks labeled 29:3 and 29:2 in the EGS145 extract (Mlut_13230-13250). The two coeluting peaks for strain EGS180 are not alkenes. This is demonstrated in the two insets in Fig. 2B, in which extracted ion chromatograms characteristic of the 29:3 and 29:2 alkenes (molecular ions at m/z 402 and 404, respectively) clearly show that these alkenes are present in the extract from strain EGS145 but are not detectable in the extract of strain EGS180 (or the negative control, strain EGS084).

To provide more information on the possible roles of the three *M. luteus* genes that, in combination, enable alkene bio-

synthesis in *E. coli*, we constructed more strains that heterologously expressed either Mlut_13240 or Mlut_13250. As summarized in Table 3, heterologous expression of Mlut_13240 or Mlut_13250 alone did not result in formation of the long-chain monoketones or alkenes observed with Mlut_13230 and Mlut_13230-13250.

In vitro studies with the purified Mlut_13230 protein. To confirm that long-chain, unsaturated monoketones observed during *in vivo* studies (Fig. 2A and 3A) derive from fatty acid condensation and that Mlut_13230 catalyzes this reaction, we conducted *in vitro* studies with N-terminally His₆-tagged Mlut_13230 protein (Table 1) and acyl-CoA (specif-

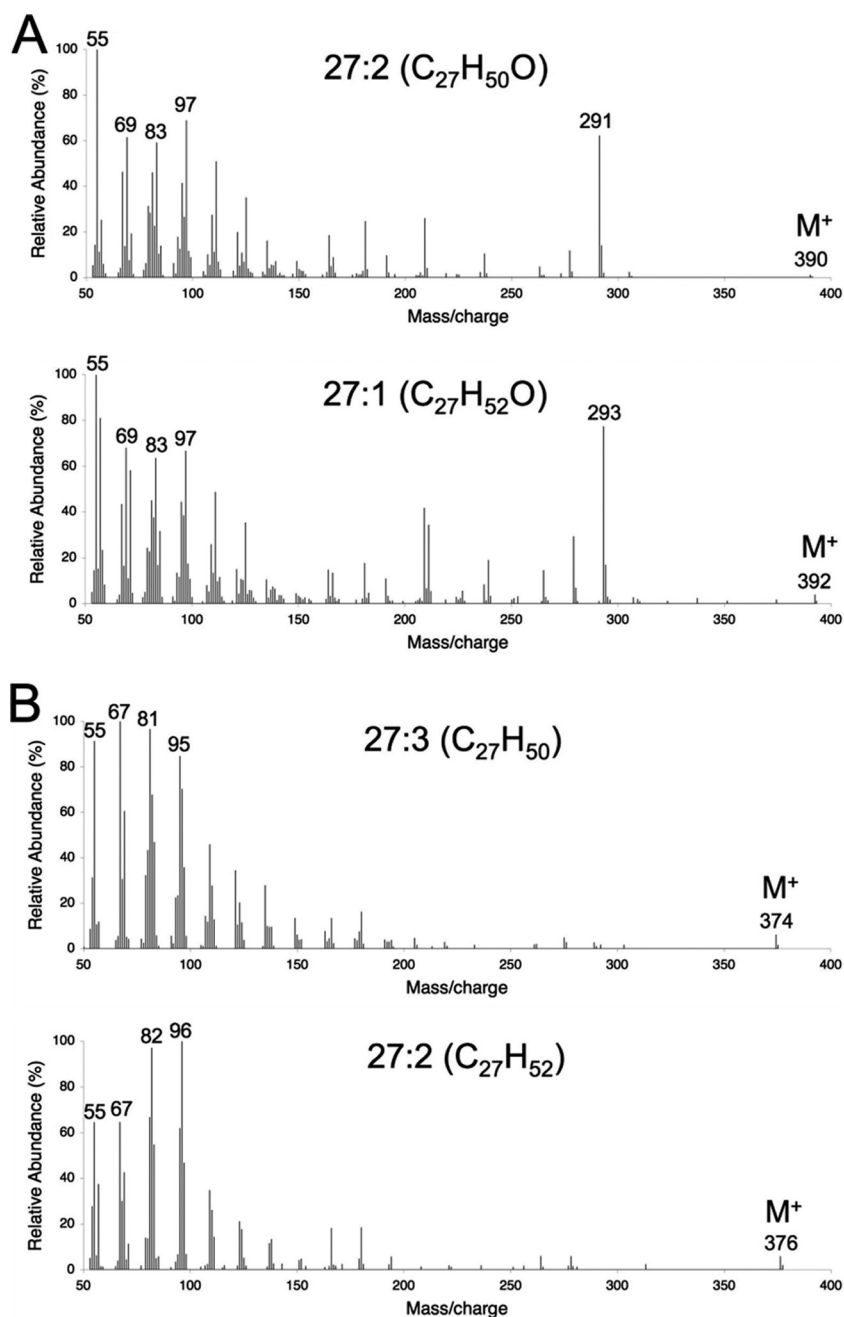


FIG. 3. (A) EI mass spectra (70 eV) of the two unsaturated C_{27} monoketones (labeled 27:2 and 27:1) in Fig. 2A. (B) EI mass spectra (70 eV) of the two C_{27} alkenes (labeled 27:3 and 27:2) in Fig. 2B.

ically, tetradecanoyl-CoA). In addition to the purified protein and acyl-CoA, the assay mixtures were amended with wild-type *E. coli* DH1 cell-free lysates, because the alkene pathway likely includes several preliminary steps that are not catalyzed by Mlut_13230 (see Discussion). Briefly, these preliminary steps may involve conversion of tetradecanoyl-CoA to 3-oxotetradecanoyl-CoA (e.g., via the early steps of β oxidation); we propose such β -ketoacyl-CoA (or -ACP) thioesters as substrates for the Mlut_13230 protein.

Assay mixtures including purified Mlut_13230 protein, tet-

radecanoyl-CoA, and DH1 lysate resulted in the formation of the same 27:2 monoketone that was prominent during *in vivo* studies of strain EGS180 (Fig. 2A and 4). Negative control assays conducted without Mlut_13230 protein or without DH1 lysate did not result in clearly detectable 27:2 monoketone (Fig. 4). These results indicate that acyl-CoAs (or their derivatives) are the source of the long-chain monoketones observed *in vivo* and that the Mlut_13230 protein is responsible for long-chain monoketone production.

To attain the necessary sensitivity for long-chain monoketone detection during *in vitro* assays, mass spectral data were

TABLE 3. Summary of long-chain alkenes and monoketones detected in *E. coli* heterologously expressing *M. luteus* genes^a

Gene(s) ^b	Strain	Alkenes produced				Monoketones produced			
		27:3 ^c	27:2	29:3	29:2	27:2	27:1	29:2	29:1
Empty vector	EGS084								
13230	EGS180					+	+	+	+
13240	EGS244								
13250	EGS300								
13230-13250	EGS145	+	+	+	+	+	+	+	+
09290 (<i>fabF</i>)	EGS210								
09310 (<i>fabH</i>)	EGS212								

^a + indicates that the compound was detected.

^b For brevity, Mlut_ has been removed from the locus tags (e.g., 13230 = Mlut_13230).

^c Number of carbon atoms:number of C=C bonds.

acquired in the SIM mode employing prominent and characteristic ions for the 27:2 monoketone (m/z 291; Fig. 3A) and the 27:1 monoketone (m/z 293; Fig. 3A). Evidence that the 27:2 monoketone peak observed in the *in vivo* studies was the same compound observed in the *in vitro* studies includes identical GC retention times and agreement of full-scan mass spectral patterns (albeit of lower quality for the *in vitro* studies because of lower concentration). The use of SIM for *in vitro* studies leaves open the possibility that additional metabolites were formed but not detected.

Long-chain alkene production and transcription of Mlut_13230-13250 in *M. luteus*. Our initial studies of *M. luteus* ATCC 4698 confirmed that it produced long-chain alkenes, which were dominated by two C₂₉ monoalkene peaks (hereafter referred to as alkene 1 and alkene 2, where alkene 1 eluted approximately 0.3 min before alkene 2 on GC/MS). For both alkene 1 and alkene 2, GC/MS analysis demonstrated a nom-

inal molecular mass of 406 Da (consistent with C₂₉H₅₈) and a fragmentation pattern characteristic of alkenes. GC-CI-TOF analysis for alkene 1 determined a molecular mass of 406.4536 Da, which is within a 0.3-mDa absolute error and a 0.7-ppm relative error of the calculated molecular mass of 406.4539 Da for C₂₉H₅₈. Similar results were obtained for alkene 2.

Alkene 2 appears to be more *anteiso* substituted than alkene 1, based upon experiments in which isoleucine was added to the growth medium. In bacteria like *M. luteus* that synthesize *iso*- and *anteiso*-branched fatty acids, isoleucine is a precursor for α -keto- β -methylvalerate, which in turn serves as a primer for *anteiso*-branched fatty acids (10, 14). When the TSB medium was amended with isoleucine (2 mM initially and 4 mM in early stationary phase), the alkene 1 concentration at 48 h was comparable to that of an unamended control (within 15%), whereas the alkene 2 concentration was more than threefold higher than in the unamended control. Thus, it seems likely that alkene 2 is *anteiso* substituted at both ends (i.e., it is the product of condensation of two *anteiso*-substituted fatty acids).

Examination of alkene 1 and 2 production throughout growth revealed that concentration trends generally corresponded to growth (optical density at 600 nm [OD₆₀₀]) and that the alkene 2/alkene 1 ratio increased considerably from late exponential phase (15 h) through early stationary phase (24 h to 48 h) (Fig. 5A). In Fig. 5A, OD₆₀₀ and alkene 1 and 2 concentrations are normalized to their maximum values, and the insets (chromatograms showing alkenes 1 and 2 at 15, 24, and 48 h) are all shown with the same y axis scale. The apparent decrease in alkene 1 and 2 concentrations between 24 and 48 h is likely a result of reduced extraction efficiency at the higher cell density at 48 h (OD₆₀₀, ~6.1) compared to 24 h (OD₆₀₀, ~2.4), rather than the result of alkene degradation, as genes associated with alkane degradation were not found in the genome. Such decreases in C₂₉ alkene concentration in postexponential phase have been observed in the related bacterium *Arthrobacter chlorophenolicus* A6 (7).

Expression of the three-gene cluster associated with alkene production (Mlut_13230-13250) generally corresponded to growth (Fig. 5B), as did C₂₉ alkene production. Transcript copy numbers for Mlut_13230, Mlut_13240, and Mlut_13250, as determined by RT-qPCR analysis, are normalized to the maximum observed value for each gene in Fig. 5B. Expression of these three genes does not appear to vary much through the period of maximum alkene production and into stationary

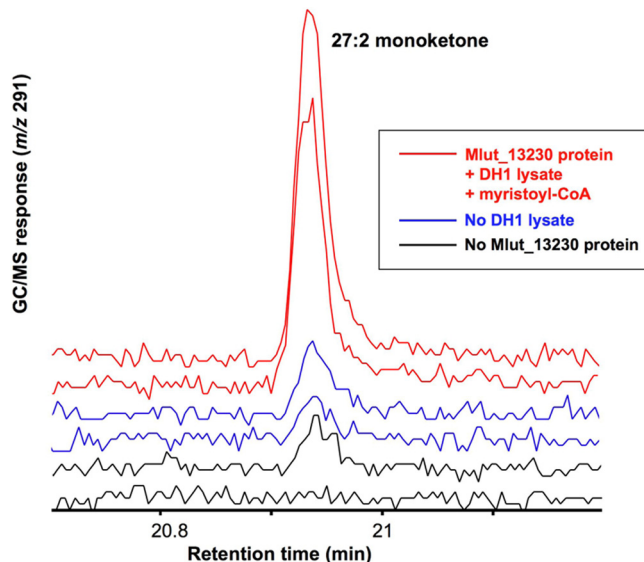


FIG. 4. Extracted ion chromatograms (m/z 291) of extracts from *in vitro* studies with purified Mlut_13230 protein. Duplicate results are shown for assays including Mlut_13230, tetradecanoyl-CoA, and crude lysate from wild-type *E. coli* DH1 (red); controls without DH1 lysate (blue); and controls without Mlut_13230 protein (black). The peak has the same retention time as the 27:2 monoketone observed during *in vivo* studies with Mlut_13230 (Fig. 2A), and m/z 291 is characteristic of that compound (Fig. 3A).

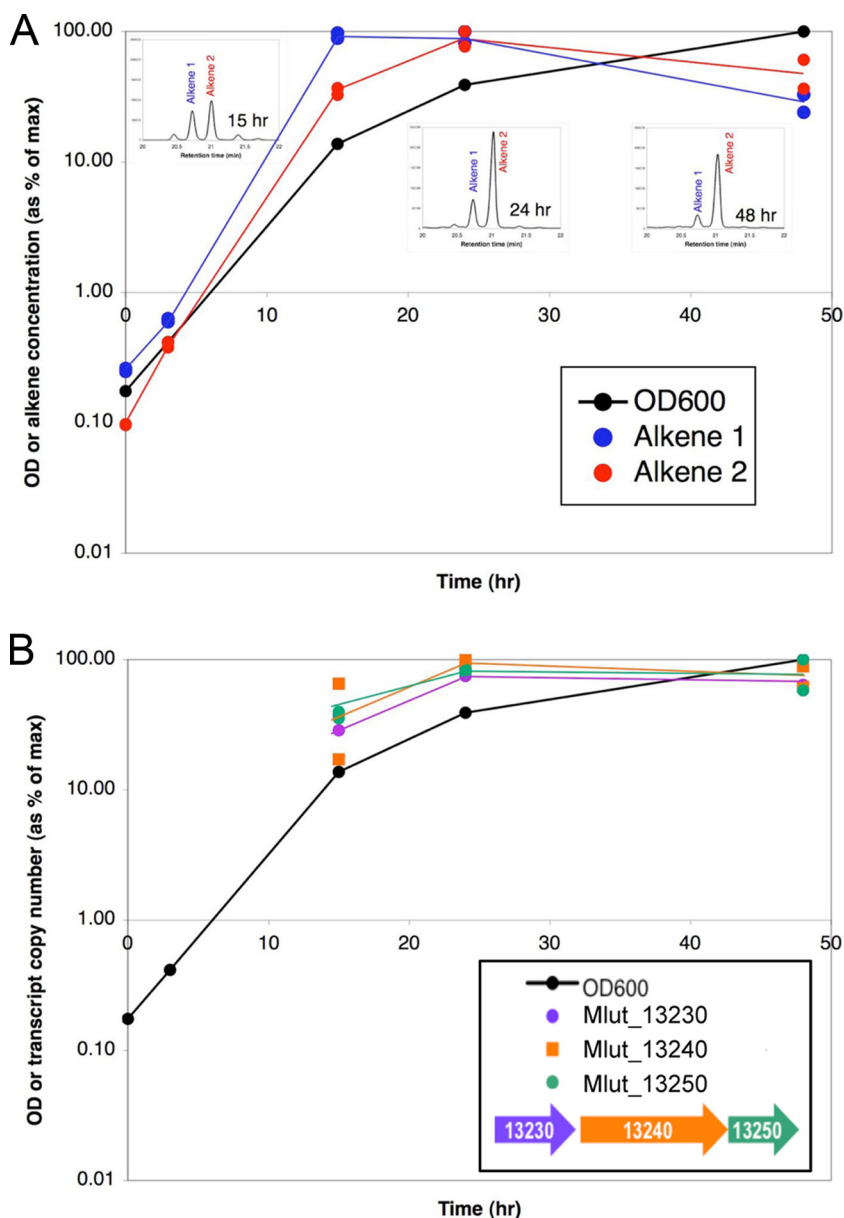


FIG. 5. Alkene production (A) and expression of alkene biosynthesis genes (B) through different growth stages of *M. luteus*. All variables are plotted as a percentage of their maximum values, and duplicate results are shown. Alkenes 1 and 2 (A) are 29:1 alkenes (see text); inset chromatograms showing the relative enhancement of alkene 2 over time are shown. In panel B, results of RT-qPCR analysis of Mlut_13230, Mlut_13240, and Mlut_13250 over time are shown.

phase. Based upon similar expression profiles for these three genes and predictions using a method described by Price and coworkers (16), it appears that Mlut_13230-13250 constitutes an operon.

DISCUSSION

We have shown that heterologous expression of three genes from *M. luteus* (Mlut_13230-13250) in a fatty acid-overproducing strain of *E. coli* resulted in production of long-chain alkenes, predominantly 27:3 and 29:3. Heterologous expression of Mlut_13230 alone produced unsaturated monoketones, predominantly 27:2, and *in vitro* studies with the purified

Mlut_13230 protein, tetradecanoyl-CoA, and wild-type *E. coli* DH1 lysate produced the same monoketone. Recently, in an international patent application (WO2008/147781), L. Friedman and B. Da Costa showed similar results for homologous genes from other bacteria. For example, heterologous expression of *oleACD* from *Stenotrophomonas maltophilia* in *E. coli* resulted in long-chain alkenes, predominantly 27:3, 27:2, 29:3, and 29:2. The four genes in *S. maltophilia* strain R551-3 that Friedman and Da Costa named *oleABCD* are apparent homologs of *M. luteus* genes featured in this study; the OleA and OleD sequences from *S. maltophilia* strain R551-3 are each 39% identical to the translated sequences of Mlut_13230 and Mlut_13250, respectively, and Mlut_13240 appears to be a

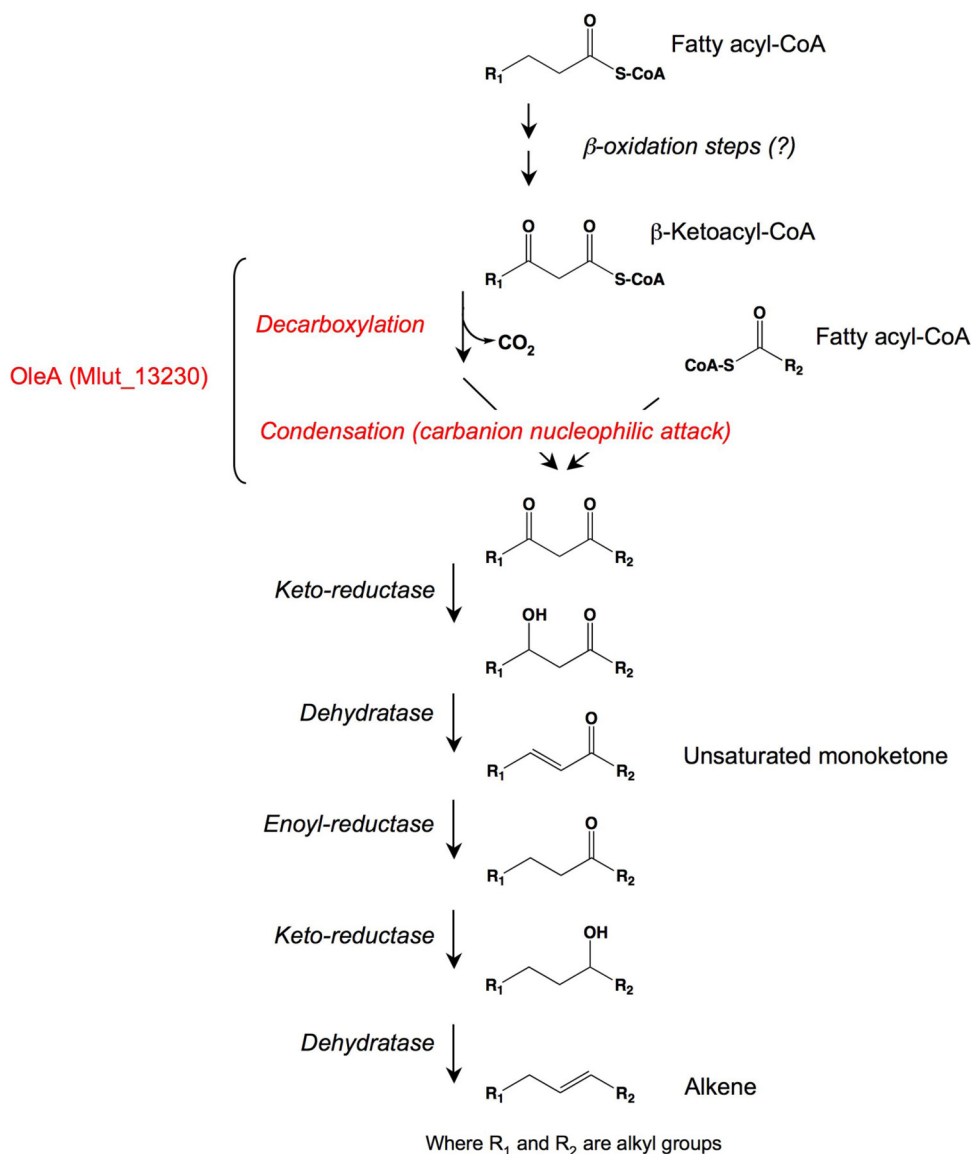


FIG. 6. Proposed pathway for alkene biosynthesis from condensation of fatty acids. Compounds shown as CoA thioesters may, in fact, be ACP thioesters. The unsaturated monoketones observed in this study (Fig. 2, 3, and 4) correspond to the metabolite following the first dehydratase reaction. In *M. luteus*, the starting compounds are likely *iso*- and *anteiso*-branched C₁₅ fatty acids and the predominant products are *iso*- and *anteiso*-branched C₂₉ monoalkenes.

fusion of *oleB* and *oleC*. Also, similar to our results for heterologous expression of Mlut_13230 in *E. coli*, Friedman and Da Costa reported that heterologous expression of *oleA* from *S. maltophilia*, *Xanthomonas axonopodis*, or *Chloroflexus aggregans* in *E. coli* resulted in predominantly 27:2, 27:1, and 27:0 monoketones. Finally, Friedman and Da Costa observed that *in vitro* studies with purified OleA, tetradecanoyl-CoA, and *E. coli* C41(DE3) lysate produced a C₂₇ monoketone. In contrast to the present study, Friedman and Da Costa did not assess heterologous expression in a Gram-negative host of *oleABCD* genes from Gram-positive bacteria (like *M. luteus*) that produce *iso*- and *anteiso*-branched fatty acids and alkenes, nor did they provide detailed evidence confirming the identity of the alkenes and monoketones, such as the GC-TOF analyses reported here.

We propose a pathway for alkene biosynthesis from fatty

acyl-CoAs (or -ACPs) that is based largely on enzyme activities homologous to those essential for fatty acid biosynthesis (Fig. 6). For brevity throughout the following discussion, we discuss CoA thioesters with the acknowledgment that ACP thioesters may actually be involved. We hypothesize that the first key step in alkene biosynthesis involves not two fatty acyl-CoAs as substrates but rather a fatty acyl-CoA and a β -ketoacyl-CoA. Thus, as suggested in Fig. 6, a fatty acyl-CoA could be converted to a β -ketoacyl-CoA by early steps of β oxidation (e.g., via an acyl-CoA dehydrogenase, an enoyl-CoA hydratase, and a 3-hydroxyacyl-CoA dehydrogenase). The first step of alkene biosynthesis in *M. luteus* (and other bacteria), catalyzed by OleA (e.g., Mlut_13230), could be decarboxylation of the β -ketoacyl-CoA and nucleophilic attack by the resulting carbanion on an acyl-CoA to form an aliphatic diketone (Fig. 6).

Such decarboxylative Claisen condensation would be consistent with the homology (Fig. 1C) of Mlut_13230 to FabH (β -ketoacyl-ACP synthase III), which catalyzes decarboxylation of malonyl-ACP and its condensation to acetyl-CoA. In fact, the FabH active-site Cys-His-Asn residues conserved in the Mlut_13230 sequence (Fig. 1C) specifically suggest catalysis of decarboxylation by OleA; based upon structural studies of FabH in *E. coli* and *Mycobacterium tuberculosis*, the conserved Cys residue has been associated with binding of the acyl intermediate and the conserved His-Asn residues are associated with decarboxylation (8, 23). Following formation of the aliphatic diketone by OleA, alkene biosynthesis could follow a series of reductase and dehydratase reactions (Fig. 6) homologous to those catalyzed by β -ketoacyl-ACP reductases (e.g., FabG), β -hydroxyacyl-ACP dehydratases (e.g., FabZ), and enoyl-ACP reductases (e.g., FabI). In addition to carbon chain length, a key characteristic that distinguishes most intermediates in the proposed alkene biosynthesis pathway from those in the fatty acid biosynthesis pathway is the absence of an ACP thioester (for intermediates following condensation).

The data presented here are consistent with, but do not prove, the pathway proposed in Fig. 6. *In vitro* studies with the purified Mlut_13230 protein (OleA), tetradecanoyl-CoA, and wild-type *E. coli* DH1 lysate produced an unsaturated C₂₇ monoketone, which would be consistent with the proposed pathway starting with two C₁₄ thioesters (e.g., decarboxylation and condensation would yield a C₂₇ compound). The need to form a β -ketoacyl-CoA as a substrate for OleA could explain why *in vitro* controls without cell lysate yielded negligible product (Fig. 4)—the relevant β -oxidation genes needed to be supplied by the lysate. The cell lysate may also explain why the monoketone was observed rather than the diketone (i.e., FabG and FabZ present in the lysate may have been able to act on the diketone and β -hydroxyketone). *In vivo* studies of heterologous expression of *oleA* (Mlut_13230) in a fatty acid-overproducing strain of *E. coli* also produced predominantly an unsaturated C₂₇ monoketone (Fig. 2), suggesting the physiological relevance of the *in vitro* studies. The C₂₉ monoketones also observed in these *in vivo* studies (Fig. 2) would be consistent with condensation of a C₁₄ and C₁₆ substrate. The predominant diunsaturated monoketone (27:2) observed in the *in vitro* and *in vivo* studies with OleA appears inconsistent with the proposed pathway, as 27:1 or 27:0 monoketones would be expected (Fig. 6). One possible explanation for the additional double bond is that two β -ketoacyl-CoAs could serve as substrates rather than one β -ketoacyl-CoA and one acyl-CoA; this would lead to the formation of a triketone and a diunsaturated monoketone following reactions analogous to those shown in Fig. 6. Our data for heterologous expression of Mlut_13230-13250 (*oleABCD*) in *E. coli* are consistent with an aliphatic monoketone being an intermediate of alkene biosynthesis. Heterologous expression of Mlut_13230-13250 (strain EGS145) resulted in 27:3 and 29:3 as the predominant alkenes, whereas expression of Mlut_13230 alone (strain EGS180) resulted in 27:2 and 29:2 monoketones. Thus, the monoketones and alkenes had the same carbon backbones but the alkenes had one additional double bond (which would be expected if the enoyl reductase in the proposed pathway was not present or active). In this light, comparison of the number of observed double bonds in these heterologous expression studies (strain EGS145) versus alkenes

produced by wild-type *M. luteus* is instructive, as *M. luteus* produces monoalkenes (29:1) and thus apparently has effective enoyl reductase activity, in contrast to strain EGS145.

Whereas multiple lines of evidence suggest that the probable role of OleA (Mlut_13230) in alkene biosynthesis is catalysis of decarboxylative Claisen condensation, the roles of OleBC (Mlut_13240) and OleD (Mlut_13250) are not clear from our data. Heterologous expression of Mlut_13240 or Mlut_13250 alone did not produce aliphatic monoketones or alkenes (Table 3). However, alkene production seems to require the expression of all three genes, Mlut_13230-13250 (Table 3). Mlut_13250 (OleD) was annotated as a nucleoside-diphosphate-sugar epimerase (GenBank), and BLASTp searches (4) of the translated Mlut_13250 sequence against the GenBank nonredundant database revealed a conserved domain of the NADB Rossmann superfamily. It is thus possible that OleD is an NADH- or NADPH-dependent reductase. As discussed previously, the Mlut_13240 gene appears to be a fusion of *oleB* and *oleC* (which are separate genes in *S. maltophilia*, studied by Friedman and Da Costa [international patent application WO2008/147781]). From BLASTp analysis, it appears that an N-terminal region of the Mlut_13240 protein is equivalent to OleB, which has homology to the alpha/beta hydrolase fold family; a C-terminal region is equivalent to OleC, which has homology to the AMP-dependent synthetase/ligase family. The role of such proteins in the proposed pathway is unclear, but it seems that an AMP-dependent synthetase/ligase would precede Claisen condensation, after which no metabolites would contain carboxylic acid or thioester moieties. Finally, it seems possible that the enoyl reductase putatively used by *M. luteus* to generate monoalkenes (Fig. 6) is encoded by a gene not included in the Mlut_13230-13250 cluster, as di- and trienes (not monoenes) were observed during heterologous expression of Mlut_13230-13250. If OleA, OleBC, and OleD do not include an enoyl reductase, and if the pathway proposed in Fig. 6 is accurate, it follows that Mlut_13250 (OleD) is a keto reductase. Further study will be required to elucidate the roles of OleA, OleBC, and OleD in alkene biosynthesis.

ACKNOWLEDGMENTS

We thank Yisheng Kang and Eric Steen (JBEI) for providing the fatty acid-overproducing *E. coli* DH1 strain; Charles Greenblatt (Hebrew University) for providing early access to the draft genome sequence of *Micrococcus luteus*; Alyssa Redding and Tanveer Batth (Functional Genomics Department, Technology Division, JBEI) for mass spectrometric analysis of protein samples; Rudy Alvarado, Vladimir Tolstikov, and Saeed Khazaie (University of California at Davis Genome Center), as well as Doug Stevens and Steven Lai (Waters Corporation), for providing GC-TOF analyses; and Taek Soon Lee and Steven Singer (JBEI) for helpful comments on the manuscript.

J.D.K. has a financial interest in LS9, Inc., and Amyris.

This work was part of the DOE Joint BioEnergy Institute (<http://www.jbei.org/>) supported by the U.S. Department of Energy, Office of Science, Office of Biological and Environmental Research, through contract DE-AC02-05CH11231 between Lawrence Berkeley National Laboratory and the U.S. Department of Energy.

REFERENCES

1. Albro, P. W. 1971. Confirmation of the identification of the major C-29 hydrocarbons of *Sarcina lutea*. *J. Bacteriol.* **108**:213–218.
2. Albro, P. W., and J. C. Dittmer. 1969. The biochemistry of long-chain, nonisoprenoid hydrocarbons. I. Characterization of the hydrocarbons of *Sarcina lutea* and the isolation of possible intermediates of biosynthesis. *Biochemistry* **8**:394–404.

3. **Albro, P. W., and J. C. Dittmer.** 1969. The biochemistry of long-chain, nonisoprenoid hydrocarbons. IV. Characteristics of synthesis by a cell-free preparation of *Sarcina lutea*. *Biochemistry* **8**:3317–3324.
4. **Altschul, S. F., T. L. Madden, A. A. Schaffer, J. Zhang, Z. Zhang, W. Miller, and D. J. Lipman.** 1997. Gapped BLAST and PSI-BLAST: a new generation of protein database search programs. *Nucleic Acids Res.* **25**:3389–3402.
5. **Beller, H. R., and A. M. Spormann.** 1997. Anaerobic activation of toluene and *o*-xylene by addition to fumarate in denitrifying strain T. *J. Bacteriol.* **179**:670–676.
6. **Fales, H. M., T. M. Jaouni, and J. F. Babashak.** 1973. Simple device for preparing ethereal diazomethane without resorting to codistillation. *Anal. Chem.* **45**:2302–2303.
7. **Frias, J. A., J. E. Richman, and L. P. Wackett.** 2009. C₂₉ olefinic hydrocarbons biosynthesized by *Arthrobacter* species. *Appl. Environ. Microbiol.* **75**:1774–1777.
8. **Heath, R. J., and C. O. Rock.** 2002. The Claisen condensation in biology. *Nat. Prod. Rep.* **19**:581–596.
9. **Ishihama, Y., Y. Oda, T. Tabata, T. Sato, T. Nagasu, J. Rappsilber, and M. Mann.** 2005. Exponentially modified protein abundance index (emPAI) for estimation of absolute protein amount in proteomics by the number of sequenced peptides per protein. *Mol. Cell. Proteomics* **4**:1265–1272.
10. **Kaneda, T.** 1991. *Iso*- and *anteiso*-fatty acids in bacteria: biosynthesis, function, and taxonomic significance. *Microbiol. Rev.* **55**:288–302.
11. **Kirchner, O., and A. Tauch.** 2003. Tools for genetic engineering in the amino acid-producing bacterium *Corynebacterium glutamicum*. *J. Biotechnol.* **104**:287–299.
12. **Ladygina, N., E. G. Dedyukhina, and M. B. Vainshtein.** 2006. A review on microbial synthesis of hydrocarbons. *Process Biochem.* **41**:1001–1014.
13. **Meselson, M., and R. Yuan.** 1968. DNA restriction enzyme from *E. coli*. *Nature* **217**:1110–1114.
14. **Oku, H., K. Fujita, T. Nomoto, K. Suzuki, H. Iwasaki, and I. Chinen.** 1998. NADH-dependent inhibition of branched-chain fatty acid synthesis in *Bacillus subtilis*. *Biosci. Biotechnol. Biochem.* **62**:622–627.
15. **Petty, K. J.** 1996. Metal chelate affinity chromatography, p. 10.11.10–10.11.24. *In* F. M. Ausubel, R. Brent, R. E. Kingston, D. D. Moore, J. G. Seidman, J. A. Smith, and K. Struhl (ed.), *Current protocols in molecular biology*. John Wiley & Sons, Inc., New York, NY.
16. **Price, M. N., K. H. Huang, E. J. Alm, and A. P. Arkin.** 2005. A novel method for accurate operon predictions in all sequenced prokaryotes. *Nucleic Acids Res.* **33**:880–892.
17. **Sambrook, J., E. F. Fritsch, and T. Maniatis.** 1989. *Molecular cloning: a laboratory manual*, 2nd ed. Cold Spring Harbor Laboratory Press, Cold Spring Harbor, NY.
18. **Steen, E. J., Y. Kang, G. Bokinsky, Z. Hu, A. Schirmer, A. McClure, S. B. del Cardayre, and J. D. Keasling.** 2010. Microbial production of fatty acid-derived chemicals from plant biomass. *Nature* **463**:559–563.
19. **Studier, F. W.** 2005. Protein production by auto-induction in high density shaking cultures. *Protein Expr. Purif.* **41**:207–234.
20. **Studier, F. W., and B. A. Moffatt.** 1986. Use of bacteriophage T7 RNA polymerase to direct selective high-level expression of cloned genes. *J. Mol. Biol.* **189**:113–130.
21. **Tornabene, T. G., E. Gelpi, and J. Oro.** 1967. Identification of fatty acids and aliphatic hydrocarbons in *Sarcina lutea* by gas chromatography and combined gas chromatography-mass spectrometry. *J. Bacteriol.* **94**:333–343.
22. **Wackett, L. P., J. A. Frias, J. L. Seffernick, D. J. Sukovich, and S. M. Cameron.** 2007. Genomic and biochemical studies demonstrating the absence of an alkane-producing phenotype in *Vibrio fischeri* M1. *Appl. Environ. Microbiol.* **73**:7192–7198.
23. **White, S. W., J. Zheng, Y. M. Zhang, and Rock.** 2005. The structural biology of type II fatty acid biosynthesis. *Annu. Rev. Biochem.* **74**:791–831.
24. **Young, M., V. Artsatbanov, H. R. Beller, G. Chandra, K. F. Chater, L. G. Dover, E.-B. Goh, T. Kahan, A. S. Kaprelyants, N. Kyrpides, A. Lapidus, S. R. Lowry, A. Lykidis, J. Mahillon, V. Markowitz, K. Mavrommatis, G. V. Mukamolova, A. Oren, J. S. Rokem, M. C. M. Smith, D. I. Young, and C. L. Greenblatt.** 30 November 2009. Genome sequence of the Fleming strain of *Micrococcus luteus*, a simple free-living actinobacterium. *J. Bacteriol.* [Epub ahead of print.] doi:10.1128/JB.01254-09.